# Cyclotron resonance study of polarons in GaAs

G. Lindemann, R. Lassnig, W. Seidenbusch, and E. Gornik
*Institut für Experimentalphysik, Universität Innsbruck, A-6020 Innsbruck, Austria*
(Received 19 July 1982; revised manuscript received 10 March 1983)

Cyclotron resonance absorption and emission experiments have been performed under hot-electron conditions. Four different Landau-level transitions are observed. From the splitting of the cyclotron-resonance lines, polaron effects are determined. Different polaron theories are applied and their validity is discussed. An accurate treatment of polaron effects is found to be necessary for the determination of the band-edge effective mass, which is determined to be $m_0^*=0.0650m$.

## I. INTRODUCTION

In polar semiconductors the motion of an electron is coupled to the polarization field of LO phonons to form a quasiparticle which is called a "polaron." Owing to this coupling the free-electron effective mass increases. The most significant effect can be observed in a magneto-optical experiment, when the energy difference between two Landau levels is comparable to the energy of an optical phonon.[1] This effect is called a resonant polaron. A strong pinning of the higher Landau level to the energy of the lowest level plus one optical phonon is observed (Fig. 1). The strength of the electron-phonon interaction depends on the dimensionless coupling constant $\alpha$ introduced by Fröhlich *et al.*[2] Most investigations on polarons have been done in strong polar materials with $\alpha$ larger than 1. For a review of polaron effects see Ref. 3. In weak polar materials, such as in III-V compounds with $\alpha \ll 1$, polaron effects are very small for energies away from the resonance. In addition, it is not easy to separate them from nonparabolicity.

The most successfully used magneto-optical methods are cyclotron resonance, transitions between different impurity levels, intraband combined resonances (cyclotron and spin-flip resonance), and interband magnetoabsorption.[4] Polar semiconductors are essentially opaque in the region of the optical-phonon energies due to the reststrahlen band. Therefore, in any experiment in which the optical transition energy and the phonon energy are comparable, the coupling effects are masked by the reststrahlen region. This disadvantage holds also for cyclotron resonance measurements, but can be avoided using a three-level method. That means the energy levels coupled by phonons are not identical with the levels coupled by the photons, so that resonant polaron phenomena can be investigated. In III-V compounds resonant polaron effects have been observed in InSb (Refs. 5–8), InAs (Refs. 9 and 10), and $Ga_xIn_{1-x}As_yP_{1-y}$ (Ref. 11). To our knowledge there exist no detailed optical investigations on polarons in GaAs.

A cyclotron resonance method based on the three-level scheme uses optical transitions between higher Landau

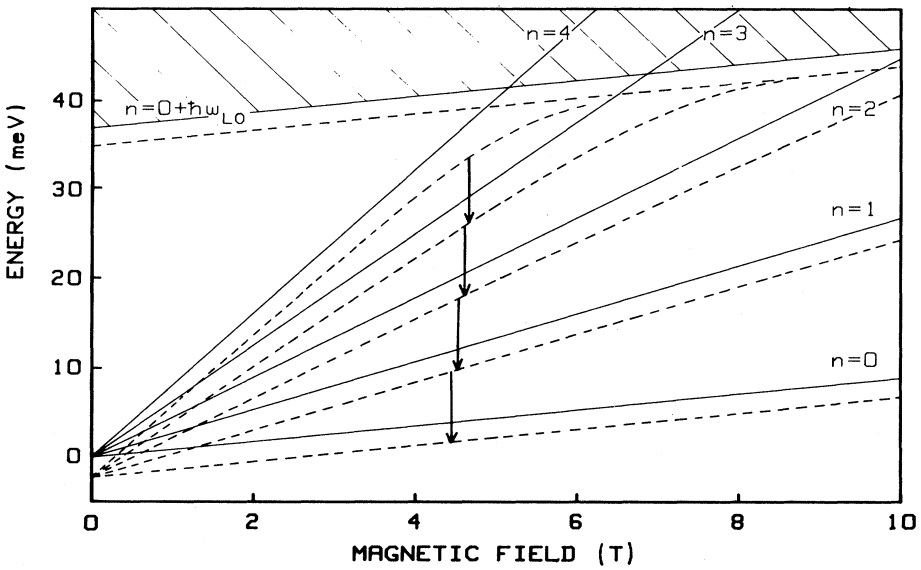


FIG. 1. Schematic diagram of the Landau levels in GaAs as a function of magnetic field. The corresponding Landau-level indices ($n$) are indicated. The solid and dashed lines are the unperturbed and perturbed levels, respectively.

 

levels. In this case the optical transitions occurs at an energy substantially smaller than the optical-phonon energy. The phonons couple the higher-energy state to the electron ground state which is not involved in the optical transition (Fig. 1). This method has been applied to InSb by Koteles and Datars.[8] They used transitions between the first and the second Landau levels to study polaron phenomena. The associated mass enhancement was calculated using Wigner-Brillouin perturbation theory.[12–14]

In the experiments presented here we report detailed magneto-optical investigations of polarons in GaAs. Cyclotron emission as well as cyclotron resonance absorption measurements are performed. Up to four lines due to transitions between different Landau levels are observed. With increasing energy the transition energy decreases and an increasing line splitting occurs. The electrons are excited by an electric field and occupy higher Landau levels in a magnetic field.

It will be shown that the splitting of the cyclotron resonance lines corresponding to different Landau-level transition energies is strongly influenced by electron-phonon coupling. This splitting is measured to high accuracy and the results are used to discuss the validity of different theories. The experimental data are compared with calculations using Wigner-Brillouin perturbation theory (WBPT), Rayleigh-Schrödinger perturbation theory (RSPT), a variational solution of the problem (VARIO) (see for example Refs. 12–14), and an improved version of WBPT (IWBPT) introduced by the authors.

## II. THEORY

Two effects modify the band structure of electrons in GaAs: polar electron–LO-phonon interaction (polarons) and nonparabolicity. Since both effects are small, they can be treated independently.[15] The unperturbed system—a parabolic band in the presence of a quantizing magnetic field—is described by a Hamiltonian $H_0$,

$$H_0=\frac{1}{2m_0^*}(\hat{p}_x-eBy)^2+\frac{1}{2m_0^*}\hat{p}_y^2+\frac{1}{2m_0^*}\hat{p}_z^2 , \tag{1}$$

with $m_0^*$ the effective band-edge mass, $(\hat{p}_x,\hat{p}_y,\hat{p}_z)$ the electron momentum operator, $\vec{r}(x,y,z)$ the electron position, and $\vec{B}$ the magnetic field. $\vec{B}$ is time independent and uniform in $z$ direction in the Landau gauge. The eigenstates of the unperturbed Hamiltonian are given by

$$H_0\,|\,n,k_z\rangle=E_n^0\,|\,n,k_z\rangle=\hbar\omega_c(n+\tfrac{1}{2})+\frac{\hbar^2k_z^2}{2m_0^*}\,|\,n,k_z\rangle . \tag{2}$$

$\omega_c=eB/m_0^*$ is the cyclotron resonance frequency, $n=0,1,2,\ldots$ is the Landau-level index, $k_z$ is the wave vector of the electrons in $z$ direction, and $|\,n,k_z\rangle$ is the wave function for the $n$th Landau level which is proportional to the harmonic oscillator eigenfunctions. With increasing magnetic field the degenerate conduction band splits into a series of equidistant Landau levels separated by an energy of $\hbar\omega_c$.

### A. Polarons

Electrons in polar crystals interact with LO phonons through the electric field of the polarization wave. This is a long-range Coulomb interaction first introduced by Fröhlich.[2] The polaron Hamiltonian is given by

$$H_p=H_0+\hbar\omega_{\rm LO}\sum_{\vec{q}} b_{\vec{q}}^{\dagger}b_{\vec{q}}+H_1=H_{0p}+H_1 , \tag{3}$$

where

$$H_1=\sum_{\vec{q}} v_q\exp(i\vec{q}\cdot\vec{r})(b_{\vec{q}}^{\dagger}+b_{-\vec{q}}) , \tag{4}$$

$$v_q^2=\frac{4\pi\alpha\hbar(\hbar\omega_{\rm LO})^{3/2}}{(2m_0^*)^{1/2}\Omega q^2} . \tag{5}$$

The first two terms of $H_p$ represent the undisturbed electron and LO-phonon system, and $H_1$ is the Fröhlich interaction between electrons and phonons. $b_{\vec{q}}^{\dagger}$ and $b_{\vec{q}}$ are creation and annihilation operators for LO phonons with wave vector $\vec{q}$ and frequency $\omega_{\rm LO}$. $\Omega$ denotes the crystal volume. The dimensionless Fröhlich coupling constant $\alpha$ can be obtained from the static and high-frequency dielectric constants.[16] From the most reliable experimental data in GaAs, $\alpha$ can be determined to $\alpha=0.058$ (Refs. 17 and 18) and $\alpha=0.068$ (Ref. 19) depending on the value of static dielectric constant employed. Owing to this small value the problem can be treated in the weak coupling limit, which means that it is sufficient to consider perturbed states containing not more than one LO phonon. The energy of an unperturbed state $|\,n,k_z;\vec{q}\,\rangle$ containing one electron in Landau level $n$ and one phonon with wave vector $\vec{q}$ is given by

$$H_{0p}\,|\,n,k_z;\vec{q}\,\rangle=(E_n^0+\hbar\omega_{\rm LO})\,|\,n,k_z;\vec{q}\,\rangle . \tag{6}$$

The band structure of electrons including polaron effects is plotted schematically in Fig. 1 as a function of the magnetic field. The solid lines show five unperturbed Landau levels corresponding to $n=0$, 1, 2, 3, and 4, and also the $k_z=0$ and the $n=0$ plus one-phonon continuum $|\,0,k_z;\vec{q}\,\rangle$. The dashed lines indicate the situation when the Fröhlich interaction is included. Generally this results in two effects: First, there is a shift of the total system by $\sim(-\alpha\hbar\omega_{\rm LO})$ independent of the magnetic field $B$; second, with increasing magnetic field the $|\,n,0\rangle$ (Ref. 20) and $|\,m,k_z;\vec{q}\,\rangle$ states mix stronger (for all $m<n$) and this interaction becomes resonant near the level crossing. As plotted in Fig. 1, the polaron states with Landau quantum number $n>0$ are repelled from the $|\,0,0;\vec{q}\,\rangle$ level and pin to it for high magnetic fields. The upper branches lying above the $|\,0,0;\vec{q}\,\rangle$ level are broadened due to the possibility of real phonon emission. Their position is not indicated in Fig. 1, since in the present work we are only interested in the position of the lower branches.

Several methods have been applied to solve the system described by the Hamiltonian equation (3): first, a variational ansatz,[21,14] which will not be discussed analytically but will be compared with the results of the other models, and second, two standard types of perturbation theory, Rayleigh-Schrödinger (RS) and Wigner-Brillouin (WB).[14] In both, the polaron Hamiltonian $H_p$ is split into $H_{0p}$, the Hamiltonian for the unperturbed system, and the perturbing potential $H_1$ [Eq. (3)]. The two procedures differ in the way in which they resolve the Schrödinger equation. In second-order perturbation theory the results for the energy corrections $\Delta E_n$ lead to very similar analytical ex-

pressions. The matrix elements are identical and only the denominators differ:

$$\Delta E_n = \sum_{m=0}^{\infty} \sum_{\vec{q}} \frac{|M_{nm}(\vec{q})|^2}{D_{nm}} , \tag{7}$$

$$M_{nm}(\vec{q}) = \langle m,k_z;\vec{q}\,|\,H_1\,|\,n,0\rangle , \tag{8}$$

where

$$D_{nm}^{\mathrm{RS}} = E_n^0 - (E_m^0 + \hbar\omega_{\mathrm{LO}}) = \hbar\omega_c(n-m) - \left[\hbar\omega_{\mathrm{LO}} + \frac{\hbar^2 q_z^2}{2m_0^*}\right] , \tag{9}$$

$$D_{nm}^{\mathrm{WB}} = (E_n^0 + \Delta E_n) - (E_m^0 + \hbar\omega_{\mathrm{LO}}) = \hbar\omega_c(n-m) - \left[\hbar\omega_{\mathrm{LO}} + \frac{\hbar^2 q_z^2}{2m_0^*} - \Delta E_n\right] . \tag{10}$$

The sums go over the phonon momentum $\vec{q}$ and the Landau quantum number $m$ of the virtual states $|\,m,k_z;\vec{q}\,\rangle$. They are converted into integrals and after some analytical integration[14] one gets

$$\Delta E_n = \frac{-\alpha\hbar\omega_{\mathrm{LO}}^{3/2}}{\sqrt{\omega_c \pi}} \int_0^{\infty} dt\, G_n(t) \exp(-\gamma_n t/\hbar\omega_c) . \tag{11}$$

Only the factor $\gamma_n$ in the exponent varies for the different models. It is equal to $\hbar\omega_{\mathrm{LO}}$ in the Rayleigh-Schrödinger model, and equal to $\gamma_n = (\hbar\omega_{\mathrm{LO}} - \Delta E_n)$ in the Wigner-Brillouin theory. The detailed matrix elements and functions $G_n(t)$ are given in the Appendix for $n = 0$–3. For $\omega_c \to 0$ the final result is

$$\Delta E_n(\omega_c = 0) = -\alpha(\hbar\omega_{\mathrm{LO}})^{3/2}/(\gamma_n)^{1/2} . \tag{12}$$

This is the constant and magnetic field independent shift due to the polaron interaction (as indicated in Fig. 1).

Both perturbation theories are not well suited to describe the polaron effect consistently in the whole range of energies. While the Rayleigh-Schrödinger theory describes the ground-state correction [Eq. (12)] quite well, it fails for the $n$th excited state when $n\omega_c \to \omega_{\mathrm{LO}}$, since then the denominator vanishes in Eq. (9) for $m = 0$. It gives good results away from the resonance, but cannot be applied near the level crossing.

The Wigner-Brillouin approach has the advantage of avoiding this difficulty: Through the self-consistent resolution of the Schrödinger equation the self-energy $\Delta E_n$ is included in the denominator [Eq. (10)]. As a consequence, no divergent behavior of the self-energy occurs and the result exhibits pinning behavior. As $\omega_c$ increases, the denominator becomes at first small for $m = 0$. At the same time $\Delta E_n$ increases (with negative sign) and thus prevents the denominator from becoming zero. The resulting total energy can not become larger than $\hbar\omega_{\mathrm{LO}} + \hbar\omega_c/2$, which acts as a pinning level. However, the calculated energy levels are not accurate. Especially the difference between the zeroth and the excited Landau levels is larger than the LO-phonon energy in the pinning region, in contradiction to the physical picture. From our analysis we can give the following explanation: The total energy of the system is shifted independent of the magnetic field. In the Wigner-Brillouin theory, however, only the energy shift $\Delta E_n$ of one level is taken into account self-consistently. This results in an effective increase of the energy separation of the level $n$ to the virtual states $|\,m,k_z;\vec{q}\,\rangle$ in the perturbation procedure. The interaction strength is effectively reduced and the pinning behavior is incorrect.

Based on this analysis, we propose another type of perturbation theory which describes consistently the polaron energy levels in the whole energy range, including the resonance region. The physical background of our improved procedure is the following: As discussed by Epstein[22] the decomposition of the total Hamiltonian in an unperturbed and a perturbed part is not unique and has to be discussed separately for any specific problem. In the polaron problem the ground state ($n = 0$) is shifted by $\Delta E_0$, which can be calculated in RSPT. Therefore, for the excited states ($n > 0$) it is reasonable to take this level as a reference for counting the energies. This corresponds to the following decomposition of $H_p$:

$$H_p = H'_{0p} + H'_1 = (H_{0p} + \Delta E_0^{\mathrm{RS}}) + (H_1 - \Delta E_0^{\mathrm{RS}}) . \tag{13}$$

Therefore, we start from an unperturbed energy

$$H'_{0p}\,|\,n,0\rangle = (E_n^0 + \Delta E_0^{\mathrm{RS}})\,|\,n,0\rangle \tag{14}$$

and resolve the Schrödinger equation in a Wigner-Brillouin-type procedure. The first-order perturbation correction is $-\Delta E_0^{\mathrm{RS}}$ and compensates the factor $\Delta E_0^{\mathrm{RS}}$ in Eq. (14). Including the second-order energy correction we obtain again a similar result as in Eq. (17), with the denominator given by

$$D_{nm}^{\mathrm{IWBPT}} = (E_n^0 + \Delta E_n) - (E_m^0 + \Delta E_0^{\mathrm{RS}} + \hbar\omega_{\mathrm{LO}}) = \hbar\omega_c(n-m) - \left[\hbar\omega_{\mathrm{LO}} + \Delta E_0^{\mathrm{RS}} - \Delta E_n + \frac{\hbar^2 q_z^2}{2m_0^*}\right] . \tag{15}$$

It can be seen that the energies of the mixing levels are both corrected, and the system is described consistently: The factor $\gamma_n$ is equal to

$$\gamma_n = (\hbar\omega_{\mathrm{LO}} + \Delta E_0^{\mathrm{RS}} - \Delta E_n)$$

in our procedure. The solution coincides with the Rayleigh-Schrödinger result for $n = 0$, and leads to the correct pinning behavior to the $\hbar\omega_c/2 + \hbar\omega_{\mathrm{LO}} + \Delta E_0^{\mathrm{RS}}$ energy level for the excited states.

It should be mentioned that our decomposition of the Schrödinger equation is not arbitrary. Since there are no resonant contributions to the self-energy of the lowest Landau level, the application of Rayleigh-Schrödinger theory is well justified for $n = 0$. For higher Landau levels the interaction becomes strong in the resonant region. Our choice of $H'_{0p}$ as the unperturbed Hamiltonian in the perturbation procedure takes into account that the best energy level, which can act as a reference for the higher levels, is the perturbed ground-state level. This is best seen in the pinning regime, where the $E_0^0 + \Delta E_0^{\mathrm{RS}} + \hbar\omega_{\mathrm{LO}}$ energy level is an upper bound for the lower polaron branches, and is uniquely determined by the possibility of real transitions above this level. This provides a unique fixing of the energy reference frame (by the decomposition of $H_p$) and leads to our improved Wigner-Brillouin model. A

similar result as that obtained in Eq. (15) has been obtained in Ref. 6 by a variational procedure including higher phonon terms.

### B. Nonparabolicity

A mixing between states of different energy bands, especially conduction and valence bands, leads to nonparabolicity of the conduction band. In this case Eq. (2) is no longer correct. With the use of a three-level model neglecting all bands except the valence and conduction bands, Kane[23] obtains the following equation:

$$E(E+E_g)(E+E_g+\Delta)-k^2P^2(E+E_g+\tfrac{2}{3}\Delta)=0 \ . \tag{16}$$

$E_g$ denotes the energy gap, $\Delta$ the spin-orbit splitting of the valence band, $k$ the absolute value of the electron wave vector, and $P$ is the momentum matrix element between states of $s$ (conduction-band) and $z$ (valence-band) symmetry:

$$P=-i\frac{\hbar}{m}\langle s\,|p_z|\,z\rangle \ , \tag{17}$$

where $m$ is the free-electron mass.

In a quantizing magnetic field $B$ this equation is modified to[24,25]

$$E(E+E_g)(E+E_g+\Delta) -P^2\left[\frac{eB}{\hbar}(2n+1)+k_z^2\right](E+E_g+\tfrac{2}{3}\Delta)\pm\tfrac{1}{3}P^2\Delta\frac{eB}{\hbar}=0 \ . \tag{18}$$

For GaAs it can be shown that the contribution of the term $E^3$ is very small and can be neglected without considerable loss of accuracy. Neglecting the small spin term and introducing the free-electron contribution by

$$E=E'-\frac{\hbar^2k^2}{2m} \ , \tag{19}$$

Vrehen[26] gets for the Landau-level band edges $E_n'$ ($k_z=0$),

$$E_n'=\hbar\omega_c(n+\tfrac{1}{2}) -\left[1-\frac{m_0^*}{m}\right]^2\left[\frac{3E_g+4\Delta+2\Delta^2/E_g}{(E_g+\Delta)(3E_g+2\Delta)}\right] \times(n+\tfrac{1}{2})^2(\hbar\omega_c)^2 \ . \tag{20}$$

The effective mass at the conduction-band edge $m_0^*$ is given by

$$\frac{1}{m_0^*}=\frac{1}{m}+\frac{2P^2}{3\hbar^2}\left[\frac{2}{E_g}+\frac{1}{E_g+\Delta}\right] \ . \tag{21}$$

The first term describes the undisturbed Landau levels corresponding to the parabolic case and the second term represents the nonparabolic correction which depends quadratically on $B$.

Another approximation is often used to solve Eq. (16). In the limit $\Delta\to\infty$ as stated by Lax,[25] or more exactly for $E\ll E_g+\Delta$ (Ref. 27), Eq. (16) results in a quadratic equation which has the following solution:

$$E_n=-\frac{E_g}{2}+\left[\left[\frac{E_g}{2}\right]^2+DE_g\right]^{1/2} \ , \qquad D=\hbar\omega_c(n+\tfrac{1}{2})+\frac{\hbar^2k_z^2}{2m_0^*}\pm\tfrac{1}{2}\mu_B\,|\,g_0^*\,|\,B \ . \tag{22}$$

The effective band-edge mass $m_0^*$ and the effective band-edge $g$ value $g_0^*$ are given by

$$\frac{1}{m_0^*}=\frac{4P^2(\Delta+\frac{3}{2}E_g)}{3\hbar^2E_g(\Delta+E_g)} \ , \tag{23}$$

$$\frac{1}{g_0^*}=-\frac{m}{m_0^*}\frac{\Delta}{\Delta+3E_g/2} \ , \tag{24}$$

and $\mu_B$ in Eq. (22) is the Bohr's magneton. The free-electron term is neglected in this approximation.

For a more accurate description of nonparabolicity in GaAs the interaction of the conduction band with higher energy bands has to be included. The problem is that the matrix elements for these interactions are not known precisely enough. The error due to the neglection of higher band contributions enters mainly in the value of the effective band-edge mass. So we use the three-level model discussed above and improve it by inserting the experimentally determined value of the band-edge mass instead of the calculated one.

We have calculated the influence of nonparabolicity according to Eqs. (20) and (22) using the following parameters: $E_g=1.52$ eV,[28] $\Delta=0.34$ eV,[28] and $g_0^*=-0.44$.[29] As the $g$ value is very small, the spin splitting is neglected. For a magnetic field of 8 T (which is the highest field used in the experiments) the cyclotron resonance energy calculated according to Eq. (20) is about 0.3% higher than that of Eq. (22). This deviation comes mainly from the free-electron-term contribution. It is important to note that this discrepancy is within the experimental uncertainty and, therefore, both approximations are equally suited to describe our experimental data. In addition, we want to point out that only differences in the Landau splittings enter our analysis, which are practically the same for all models (within a few percent).

## III. EXPERIMENTAL

The investigations were performed with high-purity $n$-type GaAs samples from different suppliers grown by liquid-phase epitaxy on semi-insulating (Cr-doped) GaAs substrates. Ohmic contacts were alloyed with In. A splitting of the cyclotron resonance into several lines due to transitions between different Landau levels is observed for all samples independent of the supplier. However, the linewidth has to be small enough so that the individual lines are separated. The linewidth is related to the square root of the ionized impurity concentration $N_I$ (Ref. 30); therefore, the experiments were done using samples with the smallest $N_I$. These samples were made out of layer R137 grown by H. Bauser (Max-Planck-Institut, Stuttgart) with a free carrier concentration of $n=1\times10^{13}$ cm$^{-3}$ and an ionized impurity concentration of $N_I=8\times10^{13}$ cm$^{-3}$. Detailed characteristics can be found in Ref. 30.

### A. Cyclotron resonance emission

The experimental system has been described in detail previously.[31] Emitter and detector are immersed in liquid He and placed in two independent magnetic fields which can be tuned separately. Cyclotron emission is generated by applying voltage pulses to the emitter. The radiation is guided by a metallic light pipe to a narrow-band photoconductive detector. The detector signal is measured using conventional boxcar techniques. The detector consists of the same GaAs material as mentioned above (R137). The narrow-band transition between the impurity levels $1s$-$2p$ ($m = +1$) of shallow impurities in a magnetic field is used for the spectral analysis. By a magnetic field up to 8 T the energy of this transition can be tuned between 36 and 110 $cm^{-1}$. The linewidth measured with a Fourier spectrometer was found to be 0.25 $cm^{-1}$.[30] In the experiments the detector line is set by a constant magnetic field to a certain resonance frequency. By tuning the emitter magnetic field the frequency of the emitted radiation is tuned through the detector line. Resonant peaks occur in the spectra whenever the emission line coincides with the detector line. Owing to the small detector linewidth we get real emission spectra with higher energies on the low emitter magnetic field side. The analysis of the spectra was performed by simulating the experimental spectra with a sum of Lorentz lines of variable positions and linewidths. The splitting of the observed lines was determined this way to high accuracy.

### B. Cyclotron resonance absorption

Cyclotron resonance transmission measurements were performed by an optically pumped far-infrared laser: The laser gas (methanol) is optically excited by a $CO_2$ laser and different wavelengths can be obtained by choosing different modes of the $CO_2$ laser.[32] The following wavelengths were used: 96.52, 118.83, 133.12, and 170.57 $\mu$m.

The radiation is guided by a metallic light pipe into the cryostat and focused on the sample by a tapered cone. The sample is placed in the center of a superconducting magnet. The transmitted radiation is guided to a broadband photoconductive detector. For wavelengths shorter than 133.12 $\mu$m we used a Ge detector doped with Ga; for longer wavelengths we used the broadband response of a GaAs detector at zero magnetic field. A cold black polyethylene filter and a linear polarizer were placed in front of the sample to reduce the influence of blackbody radiation and to avoid optical interferences.

In GaAs at 4.2 K the electrons are frozen out in the impurity ground level. By an electric field higher than the threshold for impact ionization the electrons are excited into conduction-band states. This way cyclotron resonance is switched on by an electric field, above threshold.[33] This leads to a very sensitive electromodulation method with the laser in the cw mode and the sample modulated by the electric field. Sample heating was avoided by a low-duty cycle of the applied electric field together with low laser intensities ($\mu$W).

Both emission and absorption experiments were carried out in different configurations. In Faraday configuration the electric field $\vec{E}$ was perpendicular to the magnetic field $\vec{B}$; in Voigt configuration $\vec{E}$ was parallel to $\vec{B}$. The hot-electron distribution is different for both configurations resulting in different cyclotron resonance spectra. As the carrier concentration of our samples is extremely small, plasma shifts in the cyclotron resonance are negligible.

## IV. EXPERIMENTAL RESULTS

Characteristic emission spectra as a function of the emitter magnetic field are shown for two electric fields in the $\vec{E}||\vec{B}$ configuration in Fig. 2. The detector response is set to defined frequencies of 60.4 $cm^{-1}$ (a) and of 83.4

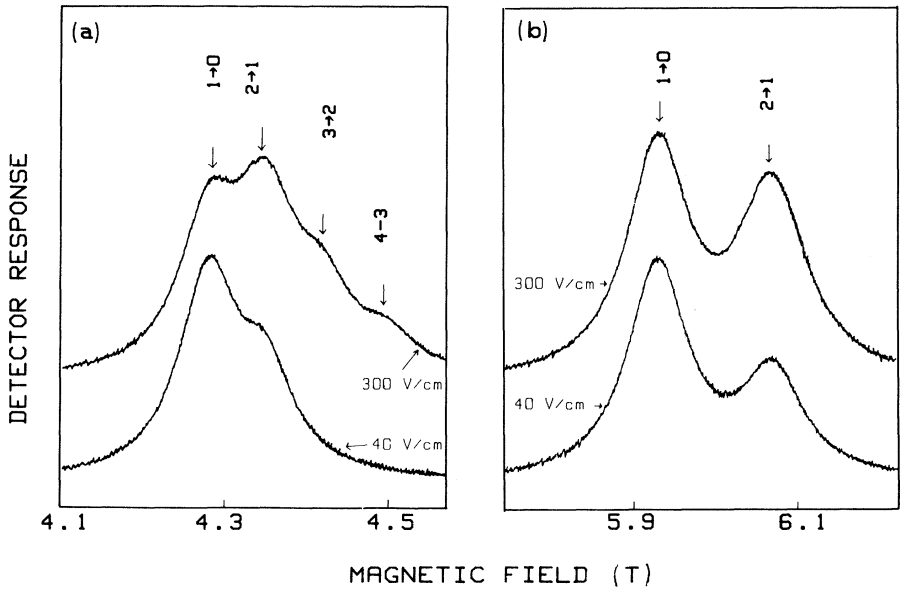


FIG. 2. Emission spectra as a function of the emitter magnetic field for two electric fields. The detector response is set to 60.4 $cm^{-1}$ (a) and 83.5 $cm^{-1}$ (b). The Landau-level indices for the individual transitions are indicated. The intensities are normalized.

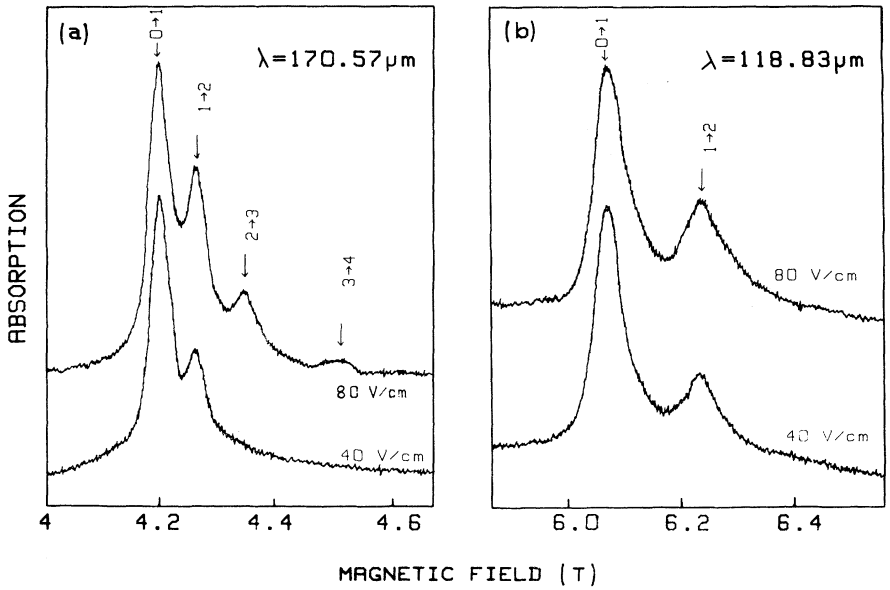


FIG. 3. Absorption spectra as a function of magnetic field for two laser wavelengths and two electric fields applied to the sample, respectively. Intensities are normalized and the corresponding Landau-level transitions are labeled.

$cm^{-1}$ (b). With increasing magnetic field the cyclotron resonance spectrum splits into several lines and the splitting of the lines increases with magnetic field. The spectra for the lower emission frequency consist of up to four lines for the higher frequency of two lines. From the increase in intensity of the additional lines with increasing electric field we conclude that these lines are due to transitions between higher Landau levels.

The corresponding Landau-level transitions are indicated. Owing to the small $g$ value in GaAs the observed splitting cannot be explained by transitions between levels of different spin orientation. The intensity of higher Landau transitions decreases with increasing magnetic field, since with increasing Landau-level energy the occupation decreases for a given excitation.

Characteristic transmission spectra as a function of magnetic field are shown for two electric fields and two laser wavelengths in the $\vec{E}||\vec{B}$ configuration in Fig. 3. As the linewidth is smaller in this case the individual Landau transitions are more clearly resolved. The results are in

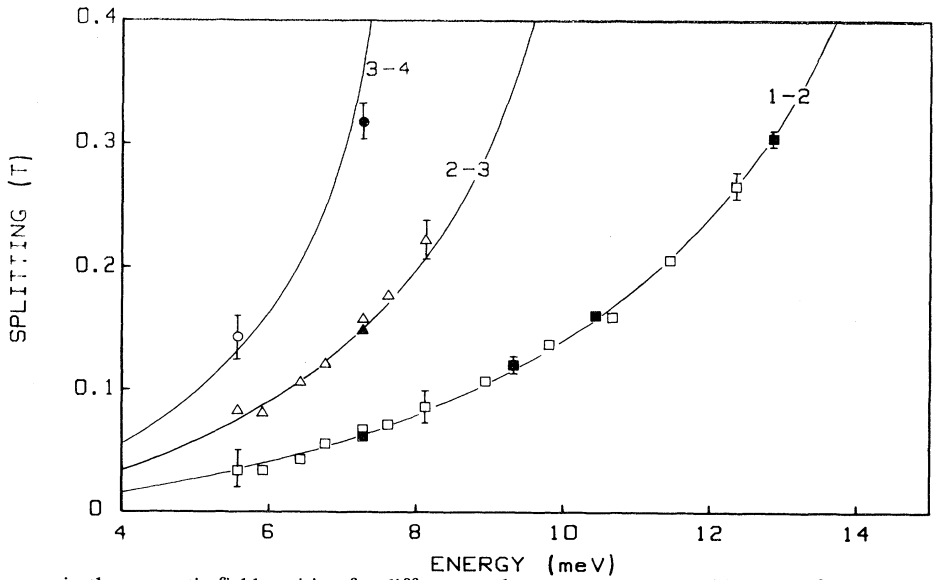


FIG. 4. Differences in the magnetic field position for different cyclotron resonance transitions as a function of the transition energy. All transitions are refered to the fundamental transition ($n=0$ to $n=1$). Different symbols correspond to different Landau-level transitions, which are labeled by the corresponding Landau-level indices. The solid curves are calculations including nonparabolicity [Eq. (22)] and polaron effects (VARIO). Transmission values are characterized by solid symbols, emission values by open symbols.

excellent agreement with the emission spectra shown above. In the $\vec{E}\perp\vec{B}$ configuration the results are almost the same, but as the heating of the electron gas is weaker, only two lines could be observed.

In the analysis the individual cyclotron resonance transitions are assumed to occur at $k_z=0$ according to the peaks in the density of states. A deviation from $k_z=0$ would result in an asymmetric line broadening of the experimental spectra due to nonparabolicity. From the absence of a considerable line broadening in the observed spectra we conclude that the assumption $k_z=0$ is justified. From the intensity ratios of the individual lines the distribution function can be determined as a function of electric field. Electron temperatures between the first and the second Landau level up to 180 K for the cases $\vec{E}||\vec{B}$ and up to 100 K for the case $\vec{E}\perp\vec{B}$ could be obtained.[34]

A splitting of the cyclotron resonance spectrum into several lines means that the Landau levels are not equidistant and the energy distance between neighboring Landau levels decreases with increasing energy, i.e., with increasing Landau quantum number. In principle, two effects can be responsible for this: nonparabolicity and coupling of electrons to polar optical phonons. To discuss the influence of these two effects we have plotted the observed line splittings of different cyclotron resonance transitions as a function of the transition energy (Fig. 4). The magnetic field position of each observed line is measured with respect to the first one. In the experiments the transition energy is fixed and determined either by the laser frequency in the absorption experiments or by the resonant energy of the detector in the emission experiments. Very good agreement is found between emission and absorption data.

From cyclotron resonance experiments the effective band-edge mass can be determined using Eq. (22). In Fig. 5 the energy of the transition from Landau level $n=0$ to $n=1$ divided by the magnetic field is plotted as a function of the magnetic field. For the parabolic case we should obtain a constant value, which is proportional to the effective mass. The data determined by cyclotron transmission measurements are more accurate, since the transition energy determined by the laser wavelength is known very precisely. The solid symbols are the experimental results. Other details of Fig. 5 will be discussed later.

## V. DISCUSSION

The cyclotron line splitting reported here is unambiguously assigned to transitions between different Landau levels. A sufficient occupation of several Landau levels, which is necessary to observe more than one cyclotron resonance line, is realized in hot-electron experiments: Extremely high electron temperatures (up to 180 K) are achieved in GaAs by electrical excitation,[34] with fields up to 500 V/cm.

The splitting of the individual cyclotron resonance transitions can be determined experimentally to high accuracy. Owing to this accuracy the validity of different polaron theories can be discussed by comparison with the experimental results.

A splitting of the cyclotron resonance line on the order of 0.5 $cm^{-1}$ at high magnetic fields has previously been observed in GaAs by several authors.[35,36] It has been explained by cyclotron resonance transitions between Landau levels of different spin orientation split due to nonparabolicity. It is important to point out that this splitting is not identical with the line splitting reported here but is about a factor of 10 smaller. In our transmission experiments at high magnetic fields we could also observe these spin-split lines, but they are not resolved very clearly.

When studying polarons in GaAs by cyclotron resonance experiments one faces the problem of how to

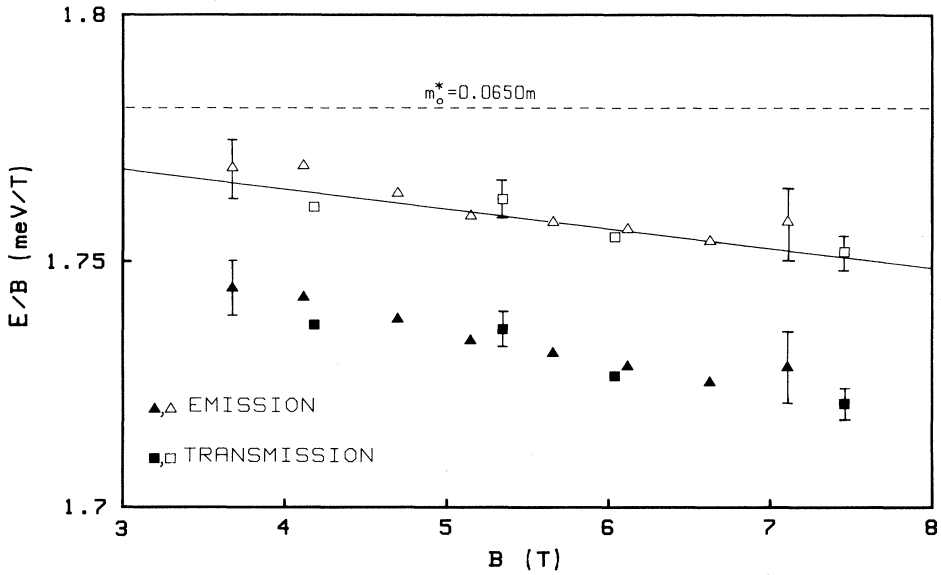


FIG. 5. Fundamental cyclotron resonance energy ($n=0$ to $n=1$) divided by the magnetic field as a function of the magnetic field. The solid symbols are the experimentally observed values, the open symbols are the same data after polaron corrections have been applied. The dashed curve represents a calculation assuming parabolic bands with $m_0^*=0.0650m$. The solid curve includes nonparabolicity [Eq. (22)] with the same effective mass.

separate the effects of nonparabolicity and electron—LO-phonon coupling. Both effects are of the same order of magnitude and lower the cyclotron resonance frequency. They only differ in the form in which they depend on energy: Nonparabolicity increases slowly and continuously with increasing energy. In contrast, the electron-phonon coupling effect which is observed in our experiments is small for low energies and becomes resonant and large near the level crossing (Fig. 1). This provides the possibility to separate the influence of the two effects.

(1) The effect of the nonparabolicity is determined from the fundamental cyclotron resonance transition energy, after substracting polaron effects.

(2) Polaron effects are determined from the shift of higher Landau-level transitions with respect to the fundamental transition after nonparabolicity has been subtracted.

*Effect (1).* Cyclotron resonance experiments are commonly used to determine the effective mass of carriers. The measured transition energies at a certain magnetic field are first corrected due to polaron effects and then compared with calculations assuming a certain band-structure model. The effective band-edge mass results as a fitting parameter. The following approximation is used to consider polaron effects away from the resonance[13]:

$$\hbar\omega_c = \hbar\omega_c^p \left[ 1 + \frac{\alpha}{6} \right], \tag{25}$$

where $\hbar\omega_c^p$ is the experimentally determined resonance energy and $\hbar\omega_c$ is the corrected resonance energy excluding polaron effects.

In Fig. 6 the calculated polaron energy correction for transitions between the lowest ($n=0$) and the first ($n=1$) Landau level is plotted as a function of $\gamma$ ($\gamma$ is defined by $\hbar\omega_c/\hbar\omega_{LO}$). The corresponding magnetic field values for GaAs are also indicated. The straight line represents the second term of Eq. (25). The upper curve is calculated by RSPT and VARIO, giving the same result.

In the calculations $\hbar\omega_{LO}$ has been taken to be 36.75 meV.[37] From Fig. 6 it can be seen that Eq. (25) is only correct for very small $\gamma$ and should not be used for values higher than $\gamma=0.1$. We think that this effect has been underestimated in some of the previously published work resulting in too large an effective band-edge mass.

In Fig. 5 we have plotted the experimentally observed transition energies for transitions between the $n=0$ and the $n=1$ Landau levels divided by the magnetic field as a function of the magnetic field. The solid symbols are the observed experimental data; the open symbols represent the same data after polaron corrections applied according to the upper curve in Fig. 6. The corrected data are now compared with calculations (solid curve) using Eq. (22). The effective band-edge mass obtained from the best fit is $m_0^*=(0.0650\pm0.005)m$ where $m$ denotes the free-electron mass. The dashed straight line corresponds to the parabolic case ($\hbar\omega_c$) with the same effective mass of $m_0^*=0.0650m$. Owing to the good agreement between experiment and theory we conclude that the model [Eqs. (20) and (22)] is sufficiently correct to describe nonparabolicity in GaAs. Herlach came to a similar result for magnetic field up to 140 T.[38]

The commonly accepted value of the effective band-edge mass in GaAs is $m_0^*=0.0665m$.[35] It is important to note that without polaron correction a fit of the experimental data (solids symbols) according to Eq. (22) leads to $m_0^*=0.0661m$, which is in reasonable agreement with the polaron Zeeman mass of Ref. 39. We conclude that the

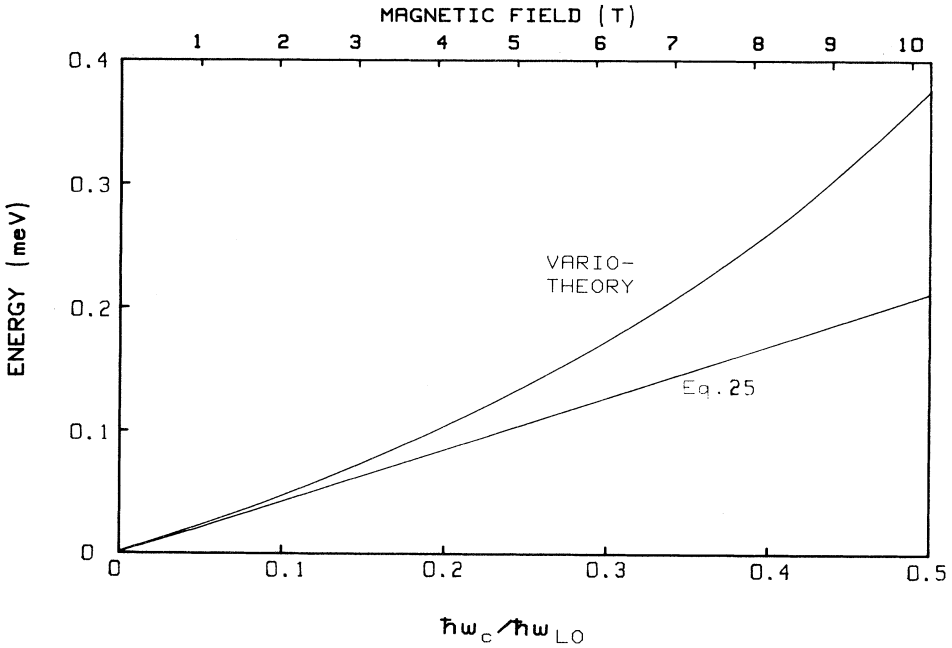


FIG. 6. Polaron energy correction to the fundamental cyclotron resonance transition as a function of $\gamma$. $\gamma$ is defined by $\gamma=\hbar\omega_c/\hbar\omega_{LO}$. The corresponding magnetic field values for GaAs are given on the top of the diagram. The straight line is calculated using Eq. (25), the upper curve by using a correct polaron theory (RSPT or VARIO, giving the same results).

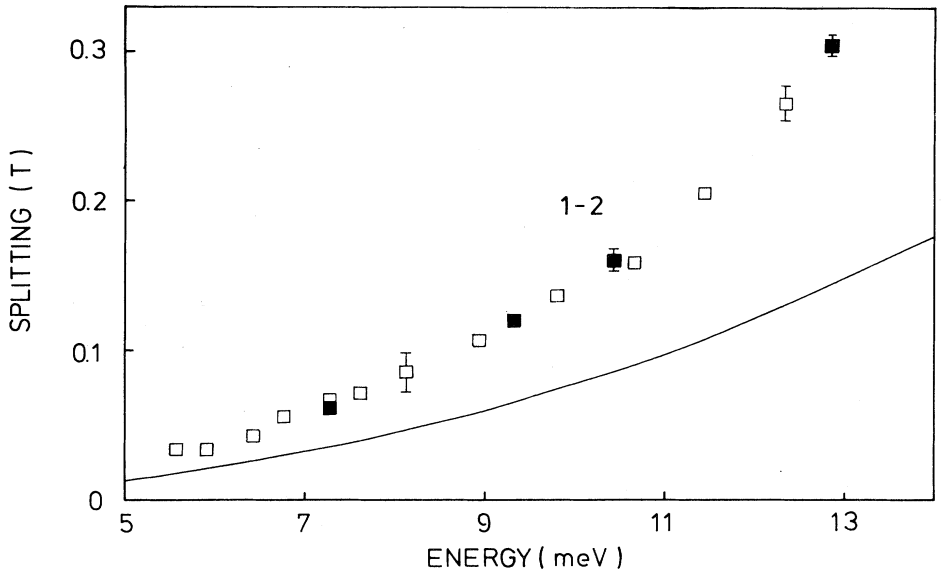


FIG. 7. Difference in magnetic field position of transitions (0-1) and (1-2) as a function of the transition energy. Transmission measurements are characterized by solid symbols, emission measurements by open symbols. The solid curve represents a calculation of the observed line splitting including nonparabolicity but not polaron effects.

difference in the effective mass compared to Ref. 35 is mainly due to our inclusion of polaron corrections.

*Effect (2).* We have calculated the splittings of the cyclotron resonance lines for different Landau-level transitions due to nonparabolicity. In Fig. 7 the calculated values of the magnetic field difference of transitions (2-1) with respect to (1-0) are compared with the corresponding experimental data (the numbers denote the Landau-level indices) as a function of the transition energy.

The observed line splitting cannot be explained only by nonparabolicity. The difference between calculations and experimental data represents the influence of polaron effects. Polaron effects are calculated using the different polaron theories discussed in the theoretical part of the present paper, with $\alpha$ as a fitting parameter. In Fig. 4 the measured splittings for all observed Landau transitions are plotted and compared with calculations including nonparabolicity and polaron effects.

The good agreement between experimental data and the calculation for all different Landau transitions using the same value of the coupling constant $\alpha$ shows that our experiments are correctly interpreted. This agreement can be achieved for all polaron theories applied. The differences between the individual theories are only manifested in different coupling constants $\alpha$ necessary for the best fit. A comparison of the resulting coupling constants $\alpha$ for the applied polaron theories is given in Table I. The most accurate values for $\alpha$ determined experimentally from the static and high-frequency dielectric constants ($\epsilon_0, \epsilon_\infty$) are also included.

A comparison of $\alpha(\epsilon_0, \epsilon_\infty)$ with $\alpha$ resulting from our calculations shows that RSPT ($\alpha=0.07$) gives the best agreement. However, this theory is only valid for energies far from resonance, and cannot be used to describe correctly resonant polaron phenomena, as discussed in the theoretical part.

From a theoretical point of view the variational model and our improved Wigner-Brillouin theory are the most reliable theories, and in contrast to the RSPT, it is valid for all energies, both far away and in the resonance. The resulting $\alpha$ values for VARIO ($\alpha=0.080$) and IWBPT ($\alpha=0.083$) are almost identical but somewhat larger than the values determined from the dielectric constants ($\alpha=0.058$, $\alpha=0.068$). It is not clear whether the origin of the small discrepancy is due to experimental uncertainties or if the polaron band bending is somewhat stronger than expected from the Fröhlich polaron theory. It is interesting to note that the $\alpha$ values determined by resonance spectroscopy in other materials are also higher than $\alpha$ determined from the dielectric constants.[8,40] In view of the smallness of the effect and the experimental problems in the determination the agreement is satisfying.

TABLE I. Comparison of the Fröhlich parameter $\alpha$ obtained from the best fit of different polaron theories to the experimental results. The most accurate literature values for $\alpha$ determined experimentally from the static and high-frequency dielectric constant ($\epsilon_0$ and $\epsilon_\infty$) are also included.

| Theory | $\alpha$ |
|---|---|
| VARIO | 0.080 |
| RSPT | 0.070 |
| WBPT | 0.130 |
| IWBPT | 0.083 |
| Expt.$(\epsilon_0, \epsilon_\infty)$[a] | 0.058 |
| Expt.$(\epsilon_0, \epsilon_\infty)$[b] | 0.068 |

[a]References 17 and 18.
[b]Reference 19.

A large discrepancy appears when the standard Wigner-Brillouin theory is applied, showing that this theory is completely unsuited to describe polaron effects in GaAs correctly. As a result we can state that polaron effects in GaAs can be well described by VARIO and by our improved Wigner-Brillouin theory. From our results we can make a few comments on the previous work of Koteles and Datars.[8] They performed similar experiments on InSb using transitions between pairs of Landau levels of different spin orientation. The observed polaron effects are compared with calculations using WBPT. Good agreement was achieved with an $\alpha$ value twice the value determined from the dielectric constants. From our analysis we can conclude that using, e.g., IWBPT instead of WBPT a more realistic value of $\alpha$ can be obtained. In addition, an improvement can be achieved by evaluating the experimental results not as a function of magnetic field but as a function of the transition energy, which is set by the laser frequency and is constant within one spectrum.

## ACKNOWLEDGMENTS

This work was sponsored by the Fonds zur Förderung der wissenschaftlichen Forschung, Austria (Projekt No. S22/05). We thank W. Zawadzki for helpful discussions.

## APPENDIX

The energy shift of the $n$th Landau level due to Fröhlich interaction is given by

$$\Delta E_n=\sum_{m=0}^{\infty}\sum_{q}\frac{|M_{nm}(q)|^2}{D_{nm}}\ . \tag{A1}$$

The denominators $D_{nm}$ for the different models are given in the text [Eqs. (9), (10), and (15)], and the matrix elements $M_{nm}(q)$ are

$$|M_{nm}(q)|^2=v_q^2\frac{e^{-a}}{m!n!}a^{(m-n)}|F_{nm}(a)|^2\ , \tag{A2}$$

$$a=q_\perp^2 l^2/2\ , \tag{A3}$$

$$F_{0m}=1\ , \tag{A4}$$

$$F_{1m}=m-a\ , \tag{A5}$$

$$F_{2m}=m(m-1)-2ma+a^2\ , \tag{A6}$$

$$F_{3m}=m^3-3m^2(1+a)+m(2+3a+3a^2)-a^3\ . \tag{A7}$$

The sums can be converted into integrals and all integrations performed analytically up to the remaining one[14]:

$$\Delta E_n=\frac{-\alpha\hbar\omega_{\rm LO}^{3/2}}{(\pi\omega_c)^{1/2}}\int_0^\infty dt\,G_n(t)\exp(-\gamma_n t/\hbar\omega_c)\ , \tag{A8}$$

where $\gamma_n$ is defined in the text and

$$G_0(t)=B(t)\ , \tag{A9}$$

$$G_1(t)=B(t)+2A(t)C(t)\ , \tag{A10}$$

$$G_2(t)=B(t)+4A(t)C(t)+6A(t)^2D(t)\ , \tag{A11}$$

$$G_3(t)=B(t)+6A(t)C(t)+18A(t)^2D(t)+\tfrac{32}{3}A(t)^3[z^2(t^{3/2}/y^3-\tfrac{9}{4}\sqrt{t}/y^2)+\tfrac{15}{8}C(t)]\ , \tag{A12}$$

$$y=1-\exp(-t),\quad z=\sqrt{t-y}\ , \tag{A13}$$

$$A(t)=[\sinh(t/2)/z]^2\ , \tag{A14}$$

$$B(t)=\ln\left[\frac{z+\sqrt{t}}{\sqrt{y}}\right]/z\ , \tag{A15}$$

$$C(t)=\sqrt{t}/y-B(t)\ , \tag{A16}$$

$$D(t)=\frac{2\sqrt{t}z^2}{9y^2}-C(t)\ . \tag{A17}$$

[1]For a review, see D. M. Larsen, in *Proceedings of the Tenth International Conference on the Physics of Semiconductors, Cambridge,* edited by S. P. Keller, J. C. Hensel, and F. Stern (U.S. AEC, Washington, D.C., 1970), p. 145.
[2]H. Fröhlich, H. Pelzer, and S. Zienau, Philos. Mag. 41, 221 (1950).
[3]*Polarons in Ionic Crystals and Polar Semiconductors,* edited by J. T. Devreese (North-Holland, London, 1972).
[4]P. G. Harper, in Ref. 3, p. 301.
[5]E. J. Johnson and D. M. Larsen, Phys. Rev. Lett. 16, 655 (1966).
[6]D. M. Larsen and E. J. Johnson, J. Phys. Soc. Jpn. Suppl. 21, 443 (1966).
[7]B. D. McCombe and R. Kaplan, Phys. Rev. Lett. 21, 756 (1968).
[8]E. S. Koteles and W. R. Datars, Phys. Rev. B 14, 1571 (1976).
[9]C. W. Litton, R. B. Dennis, and S. D. Smith, J. Phys. C 2, 2146 (1969).
[10]P. G. Harper, S. D. Smith, M. Arimondo, R. B. Dennis, and B. S. Wherrett, in *Proceedings of the Tenth International Conference on the Physics of Semiconductors, Cambridge,* edited by S. P. Keller, J. C. Hensel, and F. Stern (U.S. AEC, Washington, D.C., 1970), p. 166.
[11]R. J. Nicholas, A. M. Davidson, S. J. Sessions, and R. A. Stradling, IEEE J. Quantum Electron. QE-17, 145 (1981).
[12]D. M. Larsen, Phys. Rev. 135, A419 (1964).
[13]D. M. Larsen, Phys. Rev. 142, 428 (1966).
[14]D. M. Larsen, see Ref. 3, p. 237.
[15]B. Lax, see Ref. 3, p. 755.
[16]H. Fröhlich, Adv. Phys. 3, 325 (1954).
[17]G. E. Stillman, D. M. Larsen, C. M. Wolfe, and R. C. Brandt, Solid State Commun. 9, 2245 (1971).
[18]E. Kartheuser, see Ref. 3, p. 717.
[19]F. C. Brown, in *Polarons and Excitons,* edited by C. G. Kuper and G. D. Whitfield (Oliver and Boyd, London, 1962), p. 323.
[20]In the following we are only interested in the bottom of the Landau levels, where $k_z=0$ and the density of states is peaked.
[21]E. Haga, Prog. Theor. Phys. 13, 555 (1955).
[22]S. T. Epstein, in *Perturbation Theory and its Applications in Quantum Mechanics,* edited by C. H. Wilcox (Wiley, New York, 1966), p. 49.
[23]E. O. Kane, J. Phys. Chem. Solids 1, 249 (1957).
[24]R. Bowers and Y. Yafet, Phys. Rev. 115, 1165 (1959).
[25]B. Lax, J. G. Mavroides, H. J. Zeiger, and R. J. Keyes, Phys. Rev. 122, 31 (1961).
[26]Q. H. F. Vrehen, J. Phys. Chem. Solids 29, 129 (1968).
[27]W. Zawadzki, in *Lecture Notes in Physics,* edited by J. Ehlers

(Springer, Berlin, 1980), Vol. 133, p. 85.
[28]H. Ehrenreich, Phys. Rev. 120, 1951 (1960).
[29]C. Weisbuch and C. Hermann, Phys. Rev. B 15, 816 (1977).
[30]G. Lindemann, E. Gornik, R. Schawarz, and D. C. Tsui, in *Gallium Arsenide and Related Compounds, 1980,* edited by H. W. Thim (IOP, London, 1980), p. 631.
[31]E. Gornik, J. Magn. Magn. Mater. 11, 39 (1979).
[32]J. Heppner, C. O. Weiss, U. Hübner, and G. Schinn, IEEE J. Quantum Electron. QE-16, 392 (1980).
[33]K. L. I. Kobayashi and E. Otsuka, J. Phys. Chem. Solids 35, 839 (1974).
[34]G. Lindemann and E. Gornik, J. Phys. (Paris) C7, 399 (1981).
[35]J. M. Chamberlain, P. E. Simmonds, R. A. Stradling, and C. C. Bradley, in *Proceedings of the 11th International Conference on the Physics of Semiconductors, Warschau, 1972,* edited by M. Miasek (PWN, Warschau, 1972), p. 116.
[36]H. Fetterman, J. Waldmann, and C. M. Wolfe, Solid State Commun. 11, 375 (1972).
[37]S. Perkowitz, J. Appl. Phys. 40, 3751 (1969).
[38]F. Herlach, J. Phys. C 7, L308 (1974).
[39]G. E. Stillman, C. M. Wolf, and J. O. Dimmock, Solid State Commun. 7, 921 (1969).
[40]J. Waldman, D. M. Larsen, P. E. Tannenwald, C. C. Bradley, D. R. Cohn, and B. Lax, Phys. Rev. Lett. 23, 1033 (1969).